

A User-customized and Untethered Electro-haptic Device for Immersive Human-Machine Interaction

Ziang Cui*

ShanghaiTech University

Shanghai, China

cuiza2022@shanghaitech.edu.cn wangshy2022@shanghaitech.edu.cn zhaoyn5@shanghaitech.edu.cn

Shanyong Wang*

ShanghaiTech University

Shanghai, China

chensy2023@shanghaitech.edu.cn

Yining Zhao*

ShanghaiTech University

Shanghai, China

zhaoyn5@shanghaitech.edu.cn

Yiran Wang

Columbia University

New York, NY, USA

yw4397@columbia.edu

Xingming Wen

ShanghaiTech University

Shanghai, China

wenxm2024@shanghaitech.edu.cn

Siyuan Chen

ShanghaiTech University

Shanghai, China

chensy2023@shanghaitech.edu.cn

Ze Xiong†

ShanghaiTech University

Shanghai, China

xiongze@shanghaitech.edu.cn

Abstract—Haptic feedback is essential for human–machine interaction, as it bridges physical and digital experiences and enables immersive engagement with virtual environments. However, current haptic devices are frequently tethered, lack portability and flexibility. They also have limited ability to deliver fine-grained, multi-dimensional feedback. To address these challenges, we present a flexible, ultra-thin, and user-customized electro-haptic device fabricated with soft materials and printable liquid metal ink. Its highly integrated and lightweight design minimizes interference with natural hand movements while maintaining reliable skin contact. By delivering finely controlled electrical stimulation through 15 electrodes, it can evoke a wide range of tactile sensations that cover diverse interaction scenarios. Our user study demonstrates that the device is comfortable to wear and capable of generating tunable, precise electro-haptic feedback, thereby significantly enhancing immersion and realism in human-machine interactions.

Keywords—Electro-haptics, Wearable Devices, Flexible Electronics, Virtual Reality

I. INTRODUCTION

Human–computer interface technologies shape how people perceive, act, and stay present in digital world. A central goal of human-computer interaction is to craft truly immersive experiences that integrate not only interactive visuals and audio [1], but also the sense of touch [2]. Haptic feedback can restore contact [3], weight [4], and texture [5] cues that audio–visual channels alone cannot convey. In virtual and augmented reality (VR/AR), haptic feedback are critical for immersion and realistic human computer interaction, enabling users to control objects, infer material properties, and time their movements with greater precision [6, 7, 8].

Despite rapid progress, there are two key challenges of current haptic interfaces for immersive interaction. **1) Existing human–machine interaction interfaces are often tethered, lack portability and flexibility.** Many systems rely on rigid, bulky, or conspicuous hardware (*e.g.*, glove exoskeletons or hand-held controllers). Such designs lack portability, limit

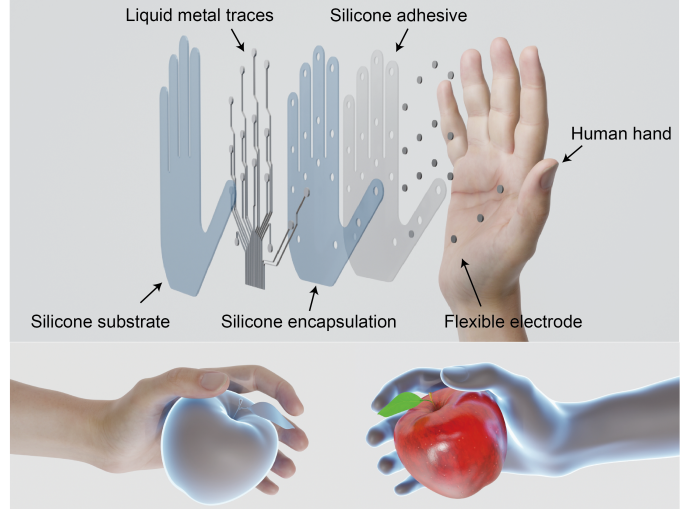


Fig. 1: Schematic diagram illustrating the structure of our electro-haptic device. Simply by capturing an image of the user’s hand, an appropriately sized model can be generated and used for device fabrication. Soft materials and printable liquid metal ink are used for flexible design. When interacting with objects in the VR environment, even though users are not physically holding anything in the real world, the electro-haptic device provides them with a realistic haptic sensation, as if they were holding actual objects in their hands.

natural hand movements, and attract unnecessary visual attention [9]. In addition, one-size-fits-all designs further ignore substantial variability in hand morphology, skin properties, and user preferences, resulting in poor fit, unstable contact, and inconsistent sensations across users and sessions [10]. **2) Current human machine interaction interface show limitations in delivering fine-grained and multi-dimensional feedback.** Much of today’s hand-worn haptic systems typically offer low spatial resolution and only a narrow dimension of sensations. Feedback is commonly uniform across broad skin regions(*e.g.*, the whole palm or all fingers) and confined

*Equal contribution. Each of them can claim to rank first.

†Corresponding author.

to a single perceptual dimension (*e.g.*, simple vibrotactile intensity), constraining designers who wish to tailor cues to diverse interaction scenarios [11, 12].

We argue that improving immersion and usability in VR/AR demands interfaces that are flexible and untethered in use while still delivering expressive feedback. To this end, we propose a hand-worn interface that integrates flexibility, portability, and spatially targeted, multi-dimensional haptic feedback. Electro-haptic is well suited to this aim, unlike mechanically actuated device rely on pressure or moving parts, electro-haptic stimulation directly excites cutaneous afferents through the skin, enabling thin, silent, and lightweight implementations [13, 14, 15]. Electro-haptics also integrates naturally with our personalization pipeline, a programmable and printable fabrication process that enables per-user customization at a low cost of only \sim 70 USD. However, conventional electrode layouts and packaging constrain wearability and customization [16], while existing control strategies often underutilize the rich perceptual space afforded by waveform parameters [13]. So in our electro-haptic device, we address these problems by employing flexible substrates with liquid metal as conductors to realize conformal and stretchable electrodes that maximize wearing comfort while maintaining stable skin contact. We further combine precise waveform modulation with a palm-wide, independently addressable electrode array to deliver spatially precise cues spanning complementary perceptual dimensions.

This work introduces a highly integrated, flexible, ultra-thin, and user-customized electro-haptic device for immersive human-machine interaction. Our approach combines a set of materials, fabrication, personalization pipelines, and system integration schemes:

- **User-customized and programmable fabrication.** Starting from a single photograph of a user’s hand, our computational pipeline estimates key anatomical landmarks and skin regions, then generates a printable electrode pattern that fits the individual’s palm. This fully programmable and rapid process enables low-cost, per-user devices without bespoke manual fitting. We employ stretchable, flexible substrates with printed liquid-metal traces to produce conformal, ultra-thin device that match the hand’s complex geometry.
- **Fine-grained and multi-dimensional electro-haptics.** Through waveform modulation, we synthesize a richer haptic vocabulary: frequency modulates temporal texture (*e.g.*, from rough/buzzy to smooth/continuous), while duty cycle adjusts perceived contact force. Coupled with spatially targeted stimulation, our system delivers multi-dimensional cues aligned with diverse interaction scenarios. We further demonstrate that our electro-haptic device could enhances task performance in VR and can serve as a effective tool for haptic augmentation.

II. RELATED WORK

A. Wearable Haptic Devices

The pursuit of realistic haptic feedback in virtual and augmented reality has led to the development of various hand-worn devices, one common form of which is the haptic glove. These systems aim to improve haptic perception of users by delivering various forms of stimulation to the hand, thereby significantly improving immersive experience. Based on their fundamental structure and the types of feedback they provide, these gloves can be broadly categorized into several types.

Vibrotactile gloves represent the most common and commercially prevalent form. They typically integrate eccentric rotating mass (ERM) motors or linear resonant actuators (LRA) into the glove design [17, 18, 19, 20, 21, 22, 23]. These actuators generate high-frequency oscillations to produce a buzzing or tapping sensation. This approach is advantageous because the technology is mature, low-cost and power-efficient, which are key attributes that make it ideal for consumer applications. However, vibrations are not very expressive. They cannot convey fine details about an object’s shape, texture, or softness because they tend to spread over a large area of the skin rather than targeting specific points precisely. Mechanical structures and manufacturing challenges also limit the density of actuators that can be integrated [19, 20]. Recent advances in materials, structures, and fabrication techniques, have enabled the development of smaller and more efficient electromagnetic actuators that can form high-density arrays for precise stimulation [24, 25].

To overcome the limitations of vibrotactile feedback, researchers have developed kinesthetic feedback gloves. These devices simulate force and resistance through mechanical structures, primarily in two forms: tendon-driven and exoskeleton systems. Tendon-driven systems use cable or similar structures to carry force, offering a lightweight and flexible design [26, 27]. Exoskeleton systems use rigid links to apply torque directly, enabling more accurate force control [28, 29]. While these systems can effectively mimic the weight and solid presence of objects, their complex mechanics often make them bulky, expensive and restrictive to natural hand movement.

In the quest for higher-fidelity touch simulation, deformable haptic gloves have been introduced. These devices create tactile sensations by producing controlled physical shapes or patterns on the skin. Pneumatic and hydraulic systems use microfluidic channels and soft actuator arrays to achieve localized deformation through precise pressure control [30, 31, 32, 33]. Piezoelectric systems use special materials to generate micron-level precision in motion output [34, 35, 36]. However, pneumatic systems require external pressure regulation units, making them large and costly. Piezoelectric solutions, on the other hand, are limited by their low force output and high cost.

In addition to the common approaches mentioned above, ultrasonic tactile stimulation [37, 38, 39] is also under exploration. Although it may enable richer stimulation patterns, it usually requires array-based ultrasonic elements and relatively

complex focusing strategies, which limits its integration into glove-based systems.

B. Electro-haptic Interfaces

Electro-haptic technology is a form of haptic feedback that directly stimulates the nervous system. It applies controlled, low-current electrical pulses to the skin, activating tactile nerve endings (such as Meissner's corpuscles and Merkel cells). This bypasses mechanical transduction and directly create sensations such as pressure, vibration, pricking, or tingling in the brain [40, 41, 42]. Unlike haptic technologies that rely on moving parts like motors or pumps, electro-haptic systems depend on precise control of electrical parameters, including amplitude, pulse width, frequency, and waveform [43]. By adjusting these parameters, various sensations can be simulated, from light touch to sustained pressure, and from fine vibrations to coarse textures [44, 45, 46].

In research on haptic gloves, several studies have focused on improving feedback resolution, and integrating multiple types of feedback. For example, Keef et al. developed a multi-modal glove that combined electrical, vibration, and thermal feedback to simulate properties like hardness, temperature, and roughness. However, the system had low electrode density and was relatively bulky [47]. Abbass et al. created a high-density electronic skin and electrode array covering the entire palm, offering accurate spatial mapping and low-latency feedback [48]. Lin and colleagues used high-frequency modulation and current steering to achieve ultra-high-resolution electro-haptic feedback (76 points/cm²) at low voltage, demonstrating applications in braille displays and VR. Still, the complex design reduced stretchability and comfort [49].

Despite progress in spatial resolution, multi-modal feedback, and low-voltage operation, most existing systems remain constrained by rigid wires and substrates, lack of personalized fit to hand anatomy, and compromises in wearability for functionality. To address these issues, this study introduces a customizable, stretchable, full-hand electro-haptic glove using liquid metal wiring. The system incorporates 15 stimulating electrodes distributed across the palm and fingers, with placements tailored to the user's hand dimensions and joint structure. This ensures broad coverage and high spatial accuracy while maintaining compatibility with natural hand movements due to the extreme flexibility and stability of liquid metal. Furthermore, an ultra-thin integrated design significantly improves comfort and natural interaction, offering a new direction for realistic, precise, and comfortable hand-based haptic interfaces.

C. Personalized Gloves Design

Personalized customization is increasingly recognized as a key requirement in the design of human-centric hardware. This trend is especially evident in wearable technologies [50], medical devices [51], and assistive systems [52], where one-size-fits-all solutions often fail to accommodate individual anatomical and ergonomic differences [53, 54]. In the context of wearable devices that rely on precise stimulation points,

even small placement errors can significantly degrade performance [55, 56]. Moreover, standardized devices frequently misalign with the user's anatomy, leading to reduced effectiveness and suboptimal user experience [57]. In wearable glove design, these misalignments highlight the need for accurate digital representations of the hand [58]. A natural response has been the use of 3D hand modeling techniques, which provide a parametric way to capture hand geometry and motion [59]. Models such as MANO [60] have become widely adopted in computer vision for tasks including hand pose estimation [61], gesture recognition [62, 63], and interaction modeling [64, 65]. Other efforts have utilized hand kinematics for exoskeleton design [66] and prosthetic customization [67]. While these approaches achieve high accuracy in geometric reconstruction, they have been primarily developed for vision and robotics applications, with limited attention to the practical needs of physical device fabrication. Our work addresses this gap by adapting hand modeling techniques specifically for personalized electro stimulation skin design, ensuring optimal stimulation point placement tailored to individual hand characteristics.

III. PERSONALIZED DESIGN ALGORITHM

We propose a novel algorithm for glove personalization that reconstructs a 3D hand model from a single RGB image. From just one photograph, the method produces both a 2D hand contour for accurate glove fitting and a 3D mesh compatible with Unity-based customization. We further evaluate its performance to demonstrate effectiveness.

A. Implementation of Personalized Design Algorithm

To acquire input data, users place their right hand flat on a surface, palm facing up, while a camera positioned about 40 centimeters above captures a square image under proper lighting. This setup ensures a clear and unobstructed view of the hand, which is essential for reliable processing [68]. The captured image is then processed by our algorithm, which extracts key features and performs the subsequent steps required for 3D reconstruction. The algorithm comprises several key steps:

1) *2D Encoding*: We first extract 2D features from the input hand image using a lightweight stacked encoder. This design reduces parameters while preserving essential geometric details.

2) *Feature Lifting*: The 2D features are lifted into 3D space through three steps:

- **Spatial Regression**: Combines heatmap encoding with position regression to improve localization accuracy and maintain temporal consistency.
- **Semantic Transformation**: Converts 2D pose features into semantically meaningful representations to describe spatial relationships between hand parts.
- **Vertex Mapping**: Uses a learnable mapping matrix to project 2D features onto 3D mesh vertices for accurate alignment.

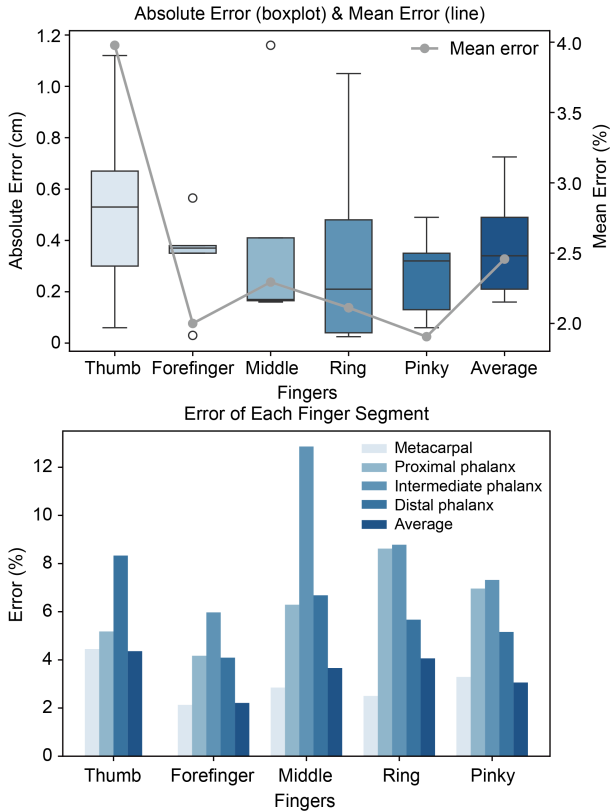


Fig. 2: Statistical evaluation of the personalized glove design algorithm. **Upper:** Absolute errors (cm) between predicted and ground-truth finger lengths, shown as boxplots for the five fingers (thumb, forefinger, middle, ring, pinky). The grey line denotes the mean error across fingers. **Lower:** Relative errors (%) for each finger, further decomposed into four anatomical segments (metacarpal, proximal phalanx, intermediate phalanx, distal phalanx) along with the averaged error.

3) 3D Decoding: We apply an efficient graph operator to reconstruct a detailed 3D hand mesh from the lifted features. The process ensures both geometric fidelity and real-time performance [69].

4) Model Fitting: The hand model is parameterized by a mesh consisting of 778 vertices and 1538 faces, providing a detailed representation of hand geometry. To improve accuracy, the reconstructed mesh is refined by fitting the joint coordinates to a reference plane and projecting the vertices accordingly, ensuring consistent geometric alignment with the real hand.

a) Joint Coordinate Regression: Given the 21 joint coordinates (20 hand joints plus one at the palm root), denoted as $\mathbf{p} = \{p_1, p_2, \dots, p_N\}$, where each $p_i \in \mathbb{R}^3$, we fit these points to a plane using a least-squares regression approach. The plane is defined by the equation: $\mathbf{n} \cdot \mathbf{p} + d = 0$, where $\mathbf{n} = (n_x, n_y, n_z)$ is the normal vector of the plane, and d is the distance from the origin to the plane.

b) Covariance Matrix and Eigenvalue Decomposition: To determine the optimal plane, we compute the centroid of the joint coordinates:

$$\mathbf{c} = \frac{1}{N} \sum_{i=1}^N \mathbf{p}_i$$

Next, we construct the covariance matrix $\mathbf{C} \in \mathbb{R}^{3 \times 3}$ as $\sum_{i=1}^N (\mathbf{p}_i - \mathbf{c})(\mathbf{p}_i - \mathbf{c})^T$. The normal vector \mathbf{n} of the plane is obtained by performing eigenvalue decomposition on \mathbf{C} . Specifically, \mathbf{n} corresponds to the eigenvector associated with the smallest eigenvalue, which minimizes the orthogonal distance from the joint points to the plane.

c) Projection of Mesh Vertices: Once the plane is determined, we project the 778 mesh vertices $\mathbf{V} = \{\mathbf{v}_1, \mathbf{v}_2, \dots, \mathbf{v}_{778}\}$ onto the plane. The projection of a vertex \mathbf{v}_i onto the plane is given by:

$$\mathbf{v}'_i = \mathbf{v}_i - (\mathbf{n} * (\mathbf{v}_i - \mathbf{c}))\mathbf{n}$$

where \mathbf{v}'_i is the projected vertex. This ensures that the final 3D model is both accurate and aligned with the physical hand. By leveraging this regression-based fitting process, we achieve a robust alignment of the hand model with the physical hand, ensuring that the 778 vertices are optimally projected onto the fitted plane.

B. Performance of Personalized Design Algorithm

To quantitatively assess the precision of the proposed personalized glove design algorithm, we performed a statistical evaluation of finger length estimation on all five fingers, as summarized in Figure 2. We collect data from the right hands of 10 volunteers (7 male and 3 female, aged 18-25, average age 21.70, SD=1.83), all of whom are right handed, and compare the predicted finger lengths of our algorithm with ground-truth measurements.

As shown in the **Upper** panel, the absolute error (cm) between predicted and ground-truth finger lengths is visualized using boxplots. The thumb exhibits the largest variability, with a mean absolute error exceeding 1 cm in certain cases, while the forefinger and pinky demonstrate relatively low error values, indicating more consistent predictions. The grey line further highlights the mean error trend across fingers, which remains below 0.5 cm for most cases, suggesting that the algorithm achieves a generally robust performance. The average error rate between five fingers is below 2.5%. The **Lower** panel provides a segment-level analysis by dividing each finger into four anatomical regions (metacarpal, proximal phalanx, intermediate phalanx, and distal phalanx). We observe that intermediate phalanx consistently yields the highest relative error, whereas metacarpal and distal phalanx show lower error rates, highlighting the algorithm's better capability in capturing proximal and distal structures.

C. Application of Personalized Design Algorithm

The personalized design algorithm addresses the limitations of traditional "one-size-fits-all" gloves by using key hand

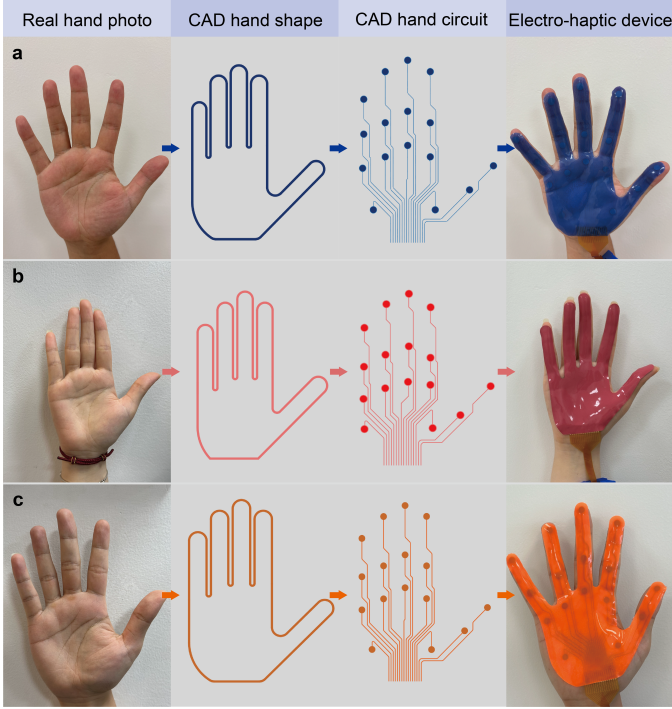


Fig. 3: Algorithmic pipeline for personalized device design. From left to right: input hand image, algorithm-extracted contour, computed stimulation sites with interconnections, and the fabricated devices applied on the hand. Examples (a–c) show three different users, their personal device shown in three different colors for easier recognition.

parameters—finger length and joint positions—to create a customized glove structure and functional layout. The algorithm begins by constructing a parametric hand model from input anthropometric data. Finger length directly determines the dimensions of the glove fingers, while the relative positions of the joints are used to algorithmically determine the placement of functional components such as electrodes and liquid metal conductive traces. Figure 3 demonstrates the application of the algorithm to produce customized device. We present three representative examples that visually convey the pipeline—from capturing the raw hand image, to contour generation and stimulation site mapping, and finally to the fabricated device applied on the hand. In summary, this method enables the simultaneous customization of glove shape and functional element placement, providing a scalable solution for producing truly personalized gloves that are both comfortable and effective.

IV. MATERIAL AND HARDWARE DESIGN

To fabricate a flexible and ultra-thin electro-haptic device, we have undertaken an optimized design from a material perspective. The core component of our approach is a printable flexible conductive ink. This printable design significantly reduces the manufacturing complexity of our device and allows for better adaptation to customized device shapes. By

combining flexible encapsulation materials and an extremely low-cost circuit control unit, we have substantially reduced the cost of the device, as well as its size (particularly thickness), weight, and fabrication difficulty. In this section, we will detail the material design, circuit design, and device implementation.

A. Design of Printable Liquid Metal Ink

In previous work, similar electrical stimulation haptic devices have utilized thin metal layers [70], metal powder-based inks [71], or polymer-based conductive coatings [72]. Although metallic materials possess certain ductility and excellent electrical conductivity, their modulus does not match that of human skin. Polymer-based conductive coatings, limited by the principle of ionic conduction, exhibit lower conductivity than metallic materials. Furthermore, their conductivity changes significantly under stretching or compression, adversely affecting the normal function of the device. Liquid metal is a fluid material with excellent metallic conductivity and high safety (very low toxicity, very low vapor pressure at room temperature) [73], making it an ideal conductive material for wearable flexible electronic devices. Compared to other metallic materials, liquid metal, being in a liquid state at room temperature, exhibits extremely high stretchability and flexibility [74]. Compared to polymer conductive materials, liquid metal offers superior conductivity ($\sim 3.4 \times 10^6 S/m$) [75]. Moreover, the conductivity of liquid metal changes very little under strain [76], making it more suitable for manufacturing flexible electronic devices. However, liquid metal inherently has very high surface tension [77], often causing it to coalesce into droplets during processing, thereby increasing the manufacturing difficulty of the device [78]. Creating high-resolution conductive patterns with liquid metal presents a challenging task.



Fig. 4: Design of printable liquid metal conductive ink. (a) Montmorillonite dispersion. (b) Liquid metal. (c) Printable liquid metal-montmorillonite conductive ink.

In our work, we employed a montmorillonite dispersion to facilitate the production of liquid metal conductive ink (as shown in the Figure 4). 2g of montmorillonite was dispersed in 20g of deionized water using an ultrasonic disruptor. Subsequently, 10g of liquid metal (EGaIn) was added, and the ultrasonic disruptor was used again to process the liquid metal into micron-sized microspheres. Through centrifugation, excess deionized water and a small amount of montmorillonite were removed, leaving the precipitated liquid metal-montmorillonite composite ink at the bottom. The ink was loaded into syringes and mounted on a pneumatic printer. By controlling the printing speed and extrusion pressure, pre-designed patterns could be printed.

In the liquid metal-montmorillonite composite ink, the liquid metal is maintained as micron-sized microspheres due to the coating of the gallium oxide shell. However, the presence of gallium oxide limits the conductivity of the composite ink; patterns printed with this composite ink are initially almost non-conductive. Heat treatment of the pattern causes the water content in the ink to evaporate, reducing the pattern's thickness, and allowing the montmorillonite and liquid metal microspheres to sediment densely. Under the sedimentation pressure from the montmorillonite, the gallium oxide shells on the liquid metal microspheres are compressed and rupture, allowing the liquid metal to re-form interconnected conductive pathways.

Through this design, we maximize the high conductivity and fluidic properties of liquid metal, processing it into a printable ink. We can pre-design the conductive pathways within the device and directly print them onto a flexible substrate using a pneumatic printer. Through a post-processing step, the ink forms well-conducting paths on the substrate.

B. Design of Electrode Material

In similar works done before, metal electrodes were widely used for sensing and stimulation on the skin surface [79]. Limited by the ductility and flexibility of metallic materials, metal electrodes often do not contact sufficiently with the skin, necessitating the application of conductive gel between the electrode and the skin to ensure good electrical contact. However, the effectiveness of the conductive gel deteriorates rapidly after short-term use [80], meaning the device cannot maintain long-term stability. Additionally, the application of conductive gel increases the difficulty of wearing the device [81]. Designing a stable, long-lasting, flexible, and conformable electrode was a significant challenge we faced.

Considering that the device encapsulation material uses silicone rubber (Smooth-On, Ecoflex 00-30), we selected a composite material consisting of conductive fillers and silicone rubber for the electrode. The silicone rubber serves as the flexible outer encapsulation matrix. The conductive materials were a combination of liquid metal and carbon nanotubes. 2g of liquid metal, 1g of carbon nanotubes, and 10g of Ecoflex 00-30 Part A were added together and mixed using a planetary mixer. Subsequently, 10g of Ecoflex 00-30 Part B was added, and the mixture was homogenized again using the planetary mixer. The well-mixed slurry was cast into a film and cured at room temperature for 4 hours. After curing, it can be cut into the required electrode shapes using a UV laser (LPKF U4) for subsequent use.

C. Wrist-worn Electro-haptic Stimulator

The wrist-worn electro-haptic stimulator adopts a minimalist design to minimize the manufacturing cost, volume, and weight of the control circuit as much as possible. It can perform boost conversion and deliver current output to 15 electrodes. Crucially, it allows for control of the current magnitude, thereby ensuring the safety of the electro-haptic feedback.

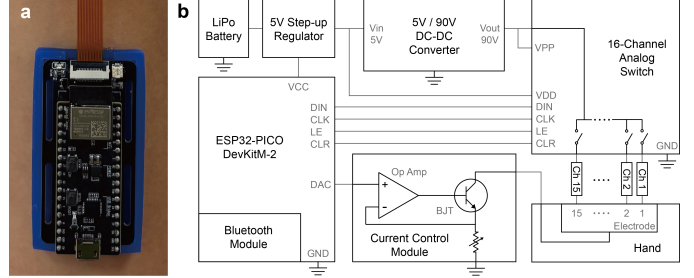


Fig. 5: The wrist-worn electro-haptic stimulator. (a) Our wrist-worn electro-haptic stimulator. (b) Schematics of our custom electro-haptic stimulator.

1) Circuit Design: The complete dimensions of our hardware circuit are 30mm × 60mm × 18mm, with a weight of only 29g. As shown in the Figure 5, we use a 3.7V lithium polymer battery to power the entire system. Through a boost regulator (PW5100, PWChip), the 3.7V input voltage is raised to 5V. The 5V voltage supplies the next stage DC-DC boost converter (LT8365, Analog Devices) and the microcontroller (ESP32-PICO-DevKitM-2, Espressif Systems). After voltage conversion, the 5V voltage is boosted to 90V to generate sufficient current for haptic perception. The microcontroller utilizes an onboard LDO chip to convert the 5V supply to the 3.3V required by the SoC chip. The microcontroller incorporates a Bluetooth module for wireless communication. The 90V high voltage is supplied to a MUX chip (TMUX9616, Texas Instruments). Under the logical control of the microcontroller, the 15 channels are selectively turned on to generate electrical stimulation haptic sensations on the hand. The current from the hand returns to the circuit through a virtual ground (VGND) electrode. The current passing through the hand is controlled by a constant current source circuit composed of an operational amplifier (LMV358) and a BJT transistor (MMBT5551).

2) Generation of Electrical Stimulation Pulses: When our microcontroller receives serial information from the host computer via the Bluetooth module, it processes the information and transmits it to the MUX to control the turning on and off of the 15 channels. Through logical control input from the microcontroller, the period and duty cycle of each pulse signal can be precisely controlled, enabling us to achieve more nuanced haptic feedback. Due to the excellent switching performance of the MUX, each channel can switch states within 1.5 microseconds, allowing us to design different pulse patterns well within the temporal recognition threshold of haptics. In our design, only one channel is active at any given time, while the others remain off during this period. This ensures better control over the haptic intensity and prevents interference between multiple channels.

3) Safety Assurance: To ensure the safe operation of the system, we use a constant current source circuit to control the magnitude of the current flowing through the hand. The microcontroller's built-in DAC outputs a control voltage to the non-inverting input of the operational amplifier. The output of the operational amplifier is connected to the base of the BJT.

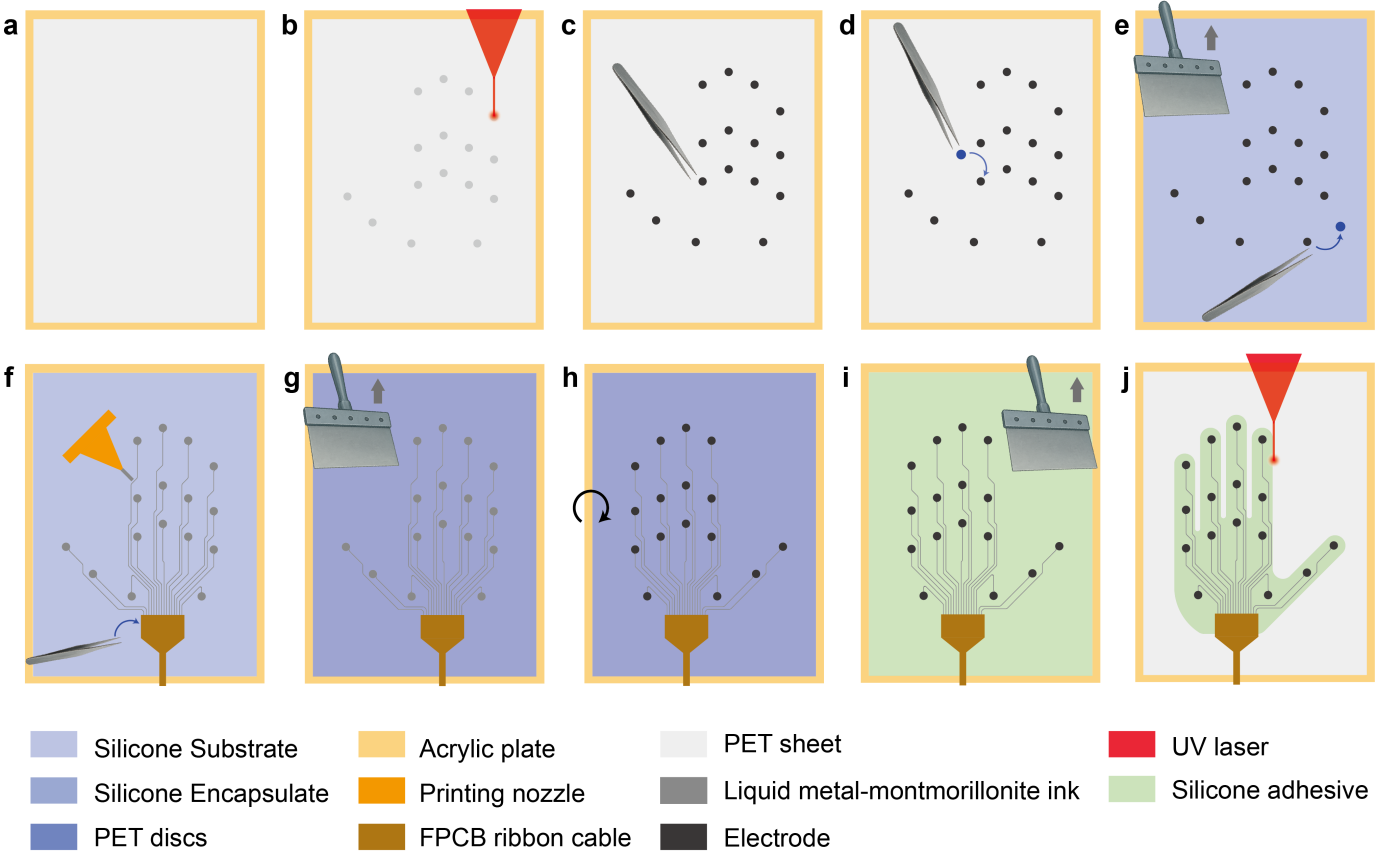


Fig. 6: Fabrication of our electro-haptic device. (a) An acrylic plate is prepared as a rigid substrate, and a thin PET sheet is attached as the flexible base layer. (b) The predefined electrode positions are marked on the surface using a UV laser. (c) Sixteen electrodes are precisely positioned on the substrate. (d) Protective PET discs are placed over each electrode. (e) A silicone layer is applied to encapsulate the electrodes while aligning the FPCB ribbon cable. (f) Conductive liquid metal–montmorillonite (LMM) ink is dispensed through a pneumatic nozzle. (g) The entire device is encapsulated. (h) The device is detached from the substrate and flipped over, with the electrode side facing upward. (i) Silicone adhesive is applied to bond the device to the skin. (j) Finally, the device is cut into a hand-shaped form using a UV laser.

The inverting input of the operational amplifier is connected to the emitter of the BJT, and the collector of the BJT is connected to the VGND electrode on the hand. A variable resistor is connected between the emitter and ground for manual adjustment of the current level. When the BJT is conducting, the voltage across the variable resistor remains constant, and the current flowing through the resistor is limited by its resistance value. Since the current from the hand can only flow through this loop, the current passing through the hand is likewise constrained to a constant value. During experiments, we set the maximum current to 3mA to ensure user safety.

V. IMPLEMENTATION OF HIGHLY INTEGRATED ELECTRO-HAPTIC DEVICE

A. Sequential Device Fabrication

Based on the device morphology design algorithm mentioned previously, a user's hand image must first be acquired. The image requirements are detailed in the earlier section.

After processing by the algorithm, the joint coordinates of the user's hand are obtained. These coordinates are used to determine information such as palm width, finger length, and electrode placement, thereby enabling the customized design of the device. Considering potential issues during fabrication, utilizing a standardized device morphology is essential. The hand was simplified into a combination of straight lines and arcs, and a CAD pattern was generated based on the hand dimension information acquired from the algorithm.

Considering the impact of hand movement on the device positioned on the palm, electrodes were placed on the fingertips, the areas of the fingers near the palm, and the finger root regions to avoid separation of the electrodes from the hand caused by motion. Based on the joint coordinates obtained from the algorithm, a CAD file specifying the electrode positions was generated. Considering the electrical connections on the device, the connection interface was uniformly designed near the base of the palm close to the wrist. Conductive trace paths were designed according to the correspondence between

electrodes and this interface. The paths must remain within the boundaries of the device morphology and avoid crossings to ensure correct device functionality. The trace paths were also generated in CAD format to facilitate subsequent printing of the conductors.

Figure 6 shows the fabrication steps of our electro-haptic device. A 0.1mm thick PET sheet was attached to an acrylic plate to serve as the substrate for device fabrication, aiding subsequent processing steps. A UV laser system was used at low power to mark the corresponding electrode positions on this substrate. The electrode material was prepared as described in the previous section, and 16 electrodes were placed at their designated positions. Pre-cut 6mm diameter PET discs were placed on top of each electrode. Subsequently, the Ecoflex 00-30 precursor was coated onto the substrate to form a 0.2mm thick film by a doctor blade. While the silicone rubber was partially cured, the PET discs on the electrodes were removed to ensure the electrode material remained uncovered.

The device was then carefully placed on the platform of a pneumatic dispenser. The pre-processed liquid metal-montmorillonite composite conductive ink was printed onto the device according to the conductor trace pattern. After printing, the device was placed in an oven at 70°C for 2 hours. This post-processing step activates the conductivity of the ink and establishes effective electrical connections with the electrodes.

Prior to applying the encapsulating layer of silicone rubber, a flexible printed circuit board (FPCB) ribbon cable was positioned at the interface area of the device, ensuring tight contact with the activated conductive traces. Similar to the previous step, the silicone rubber precursor was doctor-bladed to form a 0.2mm thick film, completely covering the entire electrode and trace region and encapsulating the upper end of the FPCB ribbon cable within the device. Notably, pigments can be added to the silicone rubber as required to meet aesthetic preferences. The silicone rubber was cured by letting it sit at room temperature for four hours.

To better secure the device to the user's hand, a skin-safe silicone adhesive (Skin Tite, Smooth-On) was selected as the adhesive layer. The device from the previous step was detached from the substrate and flipped over, placing it with the electrodes facing upwards. Analogous to earlier steps, pre-cut PET discs were placed on the electrodes, and a 0.1mm thick layer of the adhesive was doctor-bladed onto the device surface. The PET discs were then removed from the electrodes, and the assembly was left to cure for 20 minutes. Finally, the device outline was cut using a UV laser system according to the pre-designed file. The section covered by the FPCB was manually cut using a cutting knife.

The connection between the device and the custom drive system is achieved via the pre-installed FPCB ribbon cable, accommodating wrist movement. To protect the circuit system from potential failure due to factors like skin perspiration during use, it was encapsulated within a silicone rubber mold, leaving only necessary electrical connection openings exposed.

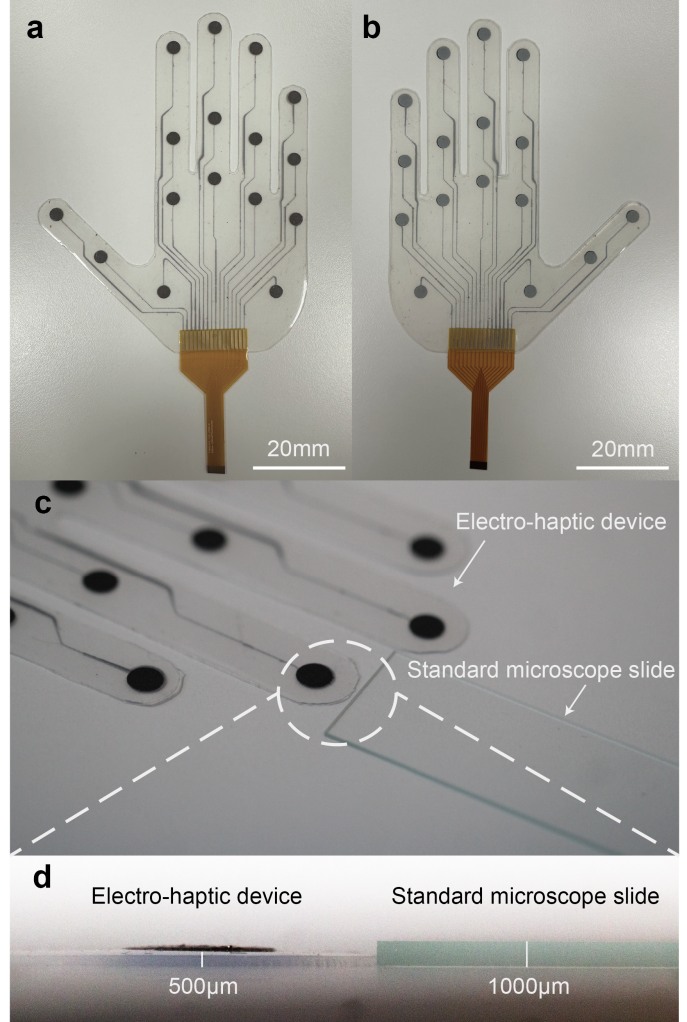


Fig. 7: Optical images of our electro-haptic device. (a, b) Fabricated device from the front and back sides. (c, d) Side view of the device, demonstrating its slim form factor. The total thickness of the device is less than that of a standard microscope slide.

Similarly, using the silicone adhesive, the circuit system can be affixed to the arm without additional fixtures, thereby avoiding any sense of restraint on the arm. The picture of our device is Figure 7. The total weight of our device is only ~48g.

B. Connect VR with Our Electro-haptic Device

Our VR application is developed with Unity3D for the Meta Quest 2 headset and incorporates real-time hand tracking. We utilize Unity's physics engine to simulate realistic physical behaviors—such as gravity, inertia—on virtual objects, enabling users to naturally grasp, release, and manipulate items within the immersive environment. To further enhance realism, the system dynamically adjusts object responses based on hand velocity and applied force, allowing subtle interactions like sliding, pushing, or tossing to feel intuitive and physically grounded. Additionally, we have implemented an improved

collision detection algorithm between the hands and virtual objects, ensuring that every contact point is captured with high spatial precision. This refinement not only prevents visual artifacts such as object penetration but also allows the system to generate accurate symbolic representations of contact events at the software layer. These signals are then transmitted as serial input to the hardware interface, enabling the connected stimulation module to respond with precise and low-latency feedback.

VI. USER STUDY #1: WEARABILITY AND INTERFERENCE OF OUR ELECTRO-HAPTIC DEVICE

A. Study Design

In this user study, we examined the impact of our electro-haptic device on users' hand-movement experiences. Common haptic feedback devices include two-handed controllers (*e.g.*, Xbox and PlayStation controllers), single-handed controllers (*e.g.*, VR controllers, Nintendo Switch Joy-Con), and glove-based haptic devices (*e.g.*, Haptic X1). Each participant was asked to experience hand movements while wearing our electro-haptic device and to compare these sensations with three conditions: bare hand, glove, and VR controller. In each trial, participants performed a series of predefined hand movements, after which they rated the difficulty and comfort of completing the actions. The study protocol was reviewed and approved by our Institutional Review Board (IRB).



Fig. 8: Comparison of participant performing hand gestures under different conditions: (a) bare hand, (b) wearing the customized device, (c) wearing a glove, and (d) gripping a VR controller.

a) Apparatus: Participants were seated comfortably and extended the dominant hand to perform gestures. As shown in Figure 8, each participant completed trials in and bare hand and three interaction devices: *bare hand (our baseline)*, *electro-haptic device worn on the palm (no current in this study)*, *regular cloth glove*, *VR handheld controller*. Participants were asked to perform five common gestures: *Thumbs-up*, *Number-one*, *Victory (V-sign)*, *OK*, and *I-love-you (ASL "ILY")*. Note that there is no electrical stimulation was delivered in this study; we isolated the effect of wearing the hardware on motor performance and perceived comfort.

b) Participants: We recruited $N = 8$ participants from our institution (5 identified as male, 3 as female; mean age 23.6, $SD = 0.74$). All were right-handed and received USD 25 compensation.

c) Procedure: We used a within-subjects design. Each participant completed 40 trials (4 conditions with 5 gestures for 2 repetitions) in randomized order. On each trial, a screen prompt indicated the target gesture; participants executed it as quickly and accurately as possible. After each trial, participants reported perceived difficulty and comfort. We recorded gesture completion (binary) and completion time (from cue onset to gesture completion). Short breaks were provided as needed.

d) Interview Protocol: After the task, we conducted a semi-structured interview to probe wearability and perceived interference. Core prompts included:

- Which condition felt *least* and *most* burdensome for executing gestures, and why?
- Relative to the bare-hand baseline, how does each condition differ?
- Specifically for our device, how does wearing it differ from the bare-hand condition?
- Would you be willing to wear this device in practice? In what scenarios and for how long?
- Do you have any additional comments about wearing our device?

B. Qualitative Feedback

a) Effects of different devices on hand movement: All eight participants ranked perceived interference across devices. Seven of eight ranked our electro-haptic device as the least interfering for producing gestures compared with bare-hand baseline, and all eight ranked the VR controller as the most interfering. Participants provided comments on our device, *e.g.*, “*It felt like a thin face mask on my hand, at first I thought it might slip, but it stayed put, so I could relax.*” (P2); “*Pretty much the same as bare hand.*” (P5). When asked about willingness to wear the device, all eight indicated participants they would be willing to wear it to obtain haptic feedback.

b) Comparisons with glove and VR controller: All eight participants noted that our electro-haptic device imposed *less* restriction on hand movement than the VR controller. Representative comments included: “*Gripping the VR controller made it hard to form the gesture.*” (P1); “*With the electro-haptic device I wasn't worried about dropping anything; with*

the controller I kept having to watch it." (P5). Six participants reported heat buildup with the glove that reduced comfort over time, "*I'd choose a glove in winter, but in summer it gets stuffy.*" (P8). One participant preferred the glove's familiarity: "*Gloves feel natural to me since I wear them in real life; a palm device keeps me aware of it and breaks immersion.*" (P7).

c) *Objective performance:* Across gestures, completion rate was 100% in both the electro-haptic device and glove conditions (Figure 8). In terms of speed, wearing our device doing gestures is slightly slower than bare hand yet substantially faster than the VR controller.

In conclusion, the qualitative reports and performance data indicate that the electro-haptic device introduces minimal interference with hand movement and remains comfortable for extended wear.

VII. USER STUDY #2: FINE-GRAINED MODULATE OF ELECTRO-HAPTIC SENSATION

A. Study Design

In this user study, we measured how square-wave frequency and duty cycle shape perceived tactile intensity. We targeted the index fingertip and asked participants to rate perceived intensity after each stimulus. We follow standard psychophysical procedures previously used to study electro-haptic perception [82]. Each trial tested one of 25 frequency-duty cycle combinations, and participants were asked to report the perceived intensity of the stimulation. The study followed a traditional psychophysical methodology, which has been widely applied in prior research on electro-haptic perception. The experimental protocol was reviewed and approved by our institutional review board (IRB).

a) *Participants:* We recruited $N = 6$ participants from our institution (3 identified as male, 3 as female; mean age 23.5, SD = 1.05). All were right-handed and received USD 25 compensation.

b) *Apparatus:* Participants were seated at a desk with their dominant hand placed palm-down on a cushioned armrest for comfort. The electro-haptic device was attached to the palm. To ensure good conductivity, participants were instructed to clean their palms with hand sanitizer followed by an alcohol wipe, and the device was attached once the hands were fully dry.

c) *Stimulus:* Electrical stimulation was delivered using conventional square-wave pulses, which targeted the index fingertip. Stimulation frequency was set to one of five fixed values (10 Hz, 25 Hz, 50 Hz, 100 Hz, 500 Hz), while duty cycle was also fixed at one of five levels (2%, 5%, 10%, 25%, 50%).

d) *Safety:* To guarantee safety during the experiment, the current amplitude was fixed at 1 mA, a value far below the minimum threshold (10 mA) known to pose potential risks to the human body [83]. Participants were not allowed to adjust either the current or the device circuitry, thereby preventing accidental changes.

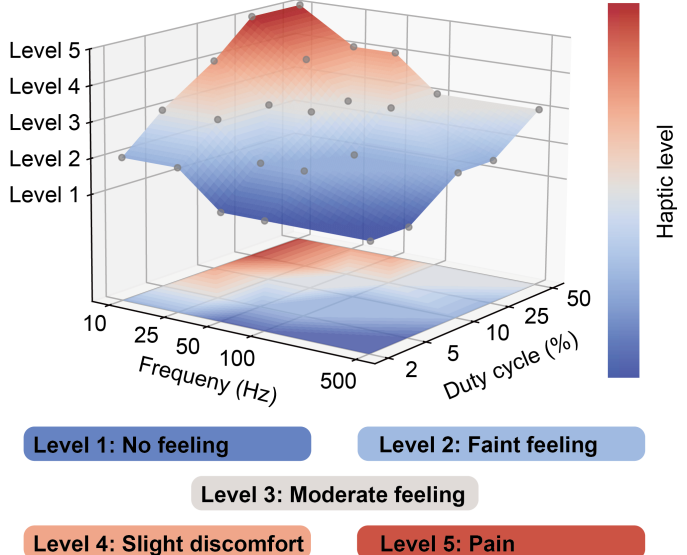


Fig. 9: Perceived electro-haptic intensity across combinations of stimulation frequency and duty cycle. The 3D surface shows mean subjective ratings on a five-level categorical scale: No feeling (Level 1), Faint feeling (Level 2), Moderate feeling (Level 3), Slight discomfort (Level 4), and Pain (Level 5). Results indicate that lower frequencies and larger duty cycles elicit stronger sensations, whereas higher frequencies and smaller duty cycles produce weaker percepts. This demonstrates that systematic modulation of temporal parameters enables fine-grained and multi-dimensional control of electro-haptic feedback.

e) *Procedure:* Each participant completed 75 trials presented in randomized order. The five frequency levels and five duty cycles formed 25 distinct test combinations, each repeated three times to ensure data reliability. Haptic sensations were classified into five categories: *No feeling*, *Faint feeling*, *Moderate feeling*, *Slight discomfort*, and *Pain*. Participants categorized each stimulation pattern according to their subjective perception.

B. Results

a) *Effect of frequency and duty cycle:* As shown in Figure 9, perceived intensity increased with larger duty cycles and decreased with higher frequencies, it means lower frequencies can make participants have stronger feelings. This pattern held consistently across participants. While absolute ratings varied between individuals for a given stimulus, there were no extreme cross-participant mismatches (e.g., one participant reporting *Pain* while another reported *No feeling* for the same stimulus).

b) *Study interpretation:* Our findings demonstrate that frequency and duty cycle offer fine-grained modulation of electro-haptic sensation beyond variations in current amplitude alone. It also shows that even with a fixed, comfortable current amplitude, systematic adjustment of these temporal parameters can elicit a wide range of perceived qualities. Specifically,

frequency primarily influences the perceived temporal texture of the stimulus, with lower frequencies producing a “buzzer” or rougher sensation and higher frequencies yielding smoother percepts, whereas duty cycle primarily alters apparent contact force, such that lower duty cycles are associated with lighter sensations, whereas higher duty cycles produce crisper and stronger impressions.

In conclusion, according to the feedback of participants, our electro-haptic device could offer fine-grained, multi-dimensional and variable electro-haptic sensation.

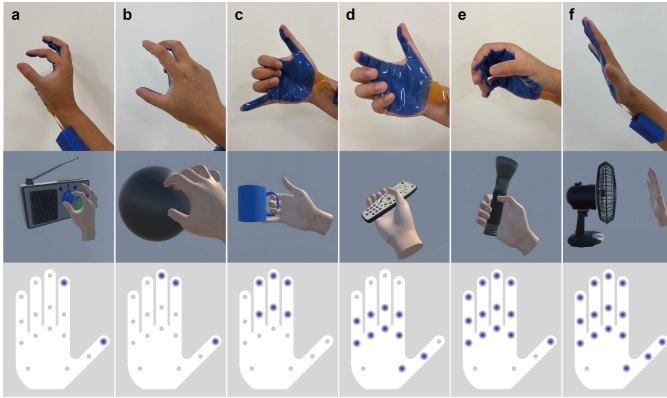


Fig. 10: Examples of hand-object interactions played in VR environments. The **top** row shows real-world grasping motions, the **middle** row illustrates the corresponding VR interactions, and the **bottom** row highlights the electrode stimulation sites on the hand. (a) Adjusting a radio knob, (b) grasping a bowling ball, (c) holding a mug, (d) holding a remote control, (e) holding a flashlight, and (f) feeling airflow from a fan.

distinct and reality tactile qualities that enhance human-object interactions.

B. Haptic Timing Cues Enhance VR Basketball Task Performance

Our electro-haptic device enables more precise and timely actions in VR, thereby increasing realism and immersion. We developed a VR free-throw mini-game (Figure 11) to evaluate how our electro-haptic device supports shooting performance. In this task, participants performed stationary shooting without dribbling—they simply picked up a virtual basketball and attempted to score. During each shot attempt, participants used their right hand to grasp the ball from below while receiving sustained, low-amplitude electro-haptic feedback indicating maintained hand-ball contact. Upon ball release, the tactile stimulation immediately ceased with a brief, distinct pulse marking the moment of hand-ball separation. The virtual ball then followed realistic physics, traveling toward the basket with appropriate momentum and trajectory based on the player’s throwing motion. After each shot attempt, regardless of whether the ball scored or missed, participants pressed a button to spawn a new basketball and reset for the next attempt. The system automatically tracked shooting performance, recording both successful scores and remaining ball count throughout each session. This design enabled players to focus entirely on shooting mechanics and aiming, using electro-haptic feedback to precisely time their grip and release without requiring visual attention to hand-ball interaction. The event-contingent electrical cues supported critical shooting parameters including grip stability and release timing, allowing users to concentrate their visual focus on the target rather than monitoring their hands.

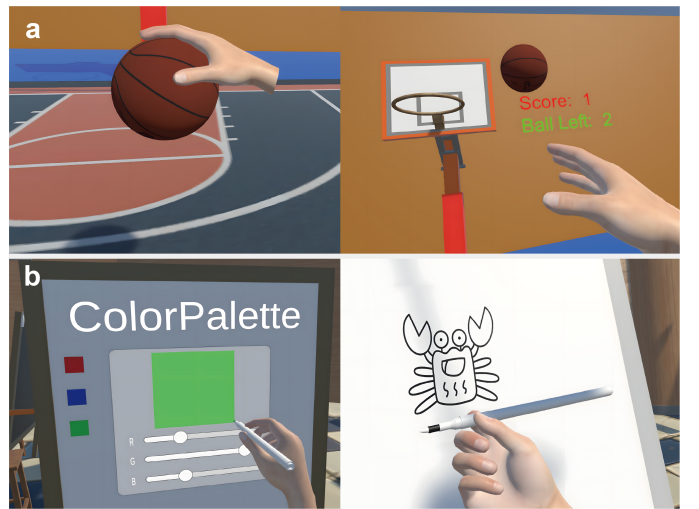


Fig. 11: Examples of two applications. (a) A basketball mini-game where users grasp and throw the ball to score. (b) A drawing interface where users select colors and sketch on a virtual canvas.

VIII. APPLICATIONS: A LIGHTWEIGHT, PERSONALIZED DEVICE FOR IMMERSIVE HAPTIC EXPERIENCES

A. Fine-grained and multi-dimensional electro-haptic feedback

One suitable testbed for our equipment is the virtual reality (VR) environment. In VR, users often rely primarily on vision to infer the state of hand-object interactions, which can increase task difficulty and diminish immersion. Most existing haptic devices provide either concentrate feedback at the fingertips or apply uniform, whole-palm stimulation due to limited haptic spatial resolution and integration. Our electro-haptic device delivers *multi-channel, location-specific* feedback across the hand, enabling more fine-grained tactile differentiation.

As illustrated in Figure 10, users interact with different virtual objects using different hand poses; stimulation sites vary accordingly with contact location and gesture. We also implemented invisible yet perceptible interaction, for example, users can feel airflow from a virtual fan on the palm even without a physical one. When the same object is approached with different gestures, the stimulated regions differ, producing

C. Haptic augmentation for VR painting

Our electro-haptic device could further function as an effective tool for haptic augmentation, broadening the range of tactile experiences. We implemented a VR painting environment (Figure 11) to explore how electro-haptic feedback enhances creative digital tasks. The virtual workspace provided three primary tools: a pen for drawing and writing, a fill tool for area coloring, and an eraser for content removal. When participants grasped the virtual pen, targeted electro-haptic stimulation was delivered to simulate realistic pen-holding posture. This tactile feedback guided users toward proper grip positioning without visual cues, supporting natural writing and drawing motions. The fill tool and eraser provided similar grip-specific feedback patterns to differentiate tool selection through touch alone. Color selection was facilitated through an RGB color palette interface where users could mix primary colors to customize both pen and fill tool outputs. The palette responded to touch interactions, allowing intuitive color sampling and tool customization during the creative process. To enhance the sense of physical interaction, all tools incorporated velocity-based force simulation. As users moved tools across the virtual canvas, the system generated speed-dependent resistance that mimicked real-world drawing dynamics—lighter, faster strokes felt smoother while deliberate, slower movements provided increased tactile resistance. This velocity-responsive feedback helped users develop natural drawing rhythms and pressure control. The painting surface consisted of a virtual whiteboard where participants could freely draw, write, and erase content. The combination of grip-specific tool feedback, color mixing capabilities, and velocity-based force simulation created a multimodal creative environment that supported both precision tasks like writing and expressive activities like artistic drawing, all while reducing dependence on visual tool monitoring.

IX. USER STUDY #3: USER'S EXPERIENCE IN APPLICATIONS

In User Studies #1 and #2, we examined how different electrical stimulation patterns shape tactile perception and assessed the comfort of wearing our electro-haptic device. In this part, we next investigated whether the feedback delivered by our device could enhance users' virtual reality (VR) interaction experience. The motivation for this study was informed by prior work exploring how wearable haptic technologies influence tactile sensation and engagement in VR environments. To this end, participants were asked to interact with virtual objects while wearing our electro-haptic device. We then conducted interviews to determine whether the electro-haptic feedback provided by our device enhanced or impeded their interactions with virtual objects.

A. Study Design

a) *Participants:* We recruited six participants (three identified as male, three as female, average age = 23.5 years, SD = 1.05) from our institution; all six participants had

partaken in our first user study; All participants were right-handed. Moreover, with the participants' consent, we videotaped and transcribed the study. Participants received USD 25 as compensation. The experimental protocol was reviewed and approved by our institutional review board (IRB).

b) *Tasks:* Participants engaged with several VR scenarios designed to evaluate electro-haptic feedback during interactive tasks. These scenarios included tactile interaction with different virtual objects, performing a VR free-throw basketball task, and engaging in a VR painting experience. Participants were free to complete all tasks at their own pace, and no fixed time limits were imposed on task completion.

c) *Interaction:* The experimental tasks were designed to ask participants to touch, grasp, or lift virtual objects while perceiving tactile feedback from our device. The task sequence was as follows: (1) In the first scenario, as shown in Figure 12, participants were instructed to interact with as many different virtual objects as possible, using a variety of hand gestures. (2) In the second scenario, as shown in Figure 13, participants picked up a basketball from the ground and attempted free-throw shots. A reset button was provided to reposition the ball, allowing multiple trials. Participants performed the task both without tactile feedback and with electro-haptic feedback enabled. (3) In the third scenario, as shown in Figure 13, participants used a virtual brush to create drawings on a digital canvas. As in the basketball task, they experienced the drawing activity under both condition (without and with tactile feedback).

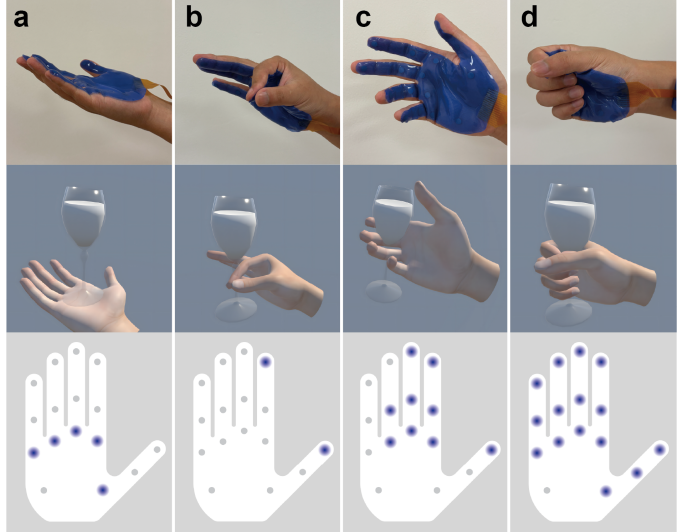


Fig. 12: **Four representative hand-object interaction gestures and their corresponding tactile feedback.** The top row shows the real hand gestures, the middle row presents the virtual interactions with a wine glass in VR, and the bottom row illustrates the mapped electro-haptic stimulation points on the hand diagram. Four gestures are: (a) Palm-up holding, (b) finger pinch, (c) open-palm grasp, and (d) full-hand grip.

d) *Apparatus:* Participants wore a Meta Quest headset along with our electro-haptic device. To ensure good conduc-

tivity, they were instructed to clean their palms with hand sanitizer followed by an alcohol wipe. After their hands were completely dry, the electro-haptic device was securely attached.

e) Procedure: Before each task, the stimulation intensity of the electro-haptic device was calibrated. The current amplitude was adjusted to the level each participant reported as most comfortable. During the experiment, the current level remained constant to ensure that all tactile sensations stayed within a comfortable range. This procedure also guaranteed participant safety throughout the study.

f) Interview: After completing each task, we conducted semi-structured interviews to explore participants' experiences of interacting with virtual objects in the VR scenarios. The interviews began with two general questions: (1) “*Can you describe your perception of the tactile feedback while interacting with virtual objects?*” and (2) “*Can you describe how burdensome it felt to perform the tasks using our electro-haptic device?*”

We then asked scenario-specific follow-up questions. For the first interaction scenario, participants were asked: “*Which object in the first scenario left the most memorable impression on you?*” For the basketball task, we asked: “*Can you describe the extent to which tactile feedback influenced your shooting performance?*” For the drawing task, participants were asked: “*Can you describe the extent to which tactile feedback increased the burden of using the VR brush?*”

In addition, for both the basketball and drawing tasks, participants were asked the same question: “*Would you prefer to use our electro-haptic device when interacting in VR scenarios?*” Finally, we concluded each interview with an open-ended question: “*Do you have any additional experiences you would like to share with us?*”

B. Qualitative Feedback

a) Tactile feedback during object interactions: Six participants directly described their experiences of interacting with virtual props. For example, one noted, “*It felt as if I were actually touching it in reality*” (P2); another remarked, “*I felt that the objects had mass, rather than being weightless*” (P3); and a third commented, “*I could perceive the shapes of the objects more clearly*” (P4). In particular, five participants emphasized that the sensation of wind from a virtual fan was especially memorable: “*In typical VR scenarios, only visible objects can be touched. With the haptic feedback device, I was able to catch the wind, which felt novel and intriguing*” (P3).

b) Tactile feedback in the basketball shooting task: All six participants reported that tactile feedback was helpful during the shooting task. Representative comments included: “*I could better sense the moment when the ball left my hand*” (P1) and “*With tactile feedback, I felt I could control the ball more effectively*” (P3). We compared participants' performance across the last five shots without tactile feedback and the last five shots with tactile feedback (see Fig.). Overall, the presence of tactile feedback improved shooting accuracy.



Fig. 13: **Two scenarios for User Study #3.** (a) Basketball mini-game: Basketball shooting game via VR headset and electro-haptic device. (b) Drawing interface: Writing and drawing tasks via VR headset and electro-haptic device.

However, due to the inherent difficulty of the task, some variability in individual performance was observed.

c) Tactile feedback in the drawing task: Five participants noted that tactile feedback made the drawing process feel more realistic. For instance, one commented, “*I felt greater control over the brush*” (P2), while another remarked, “*I could sense the roughness of the canvas*” (P6). As P4 explained, “*Without tactile feedback, it was difficult to judge the distance between the brush and the canvas; the feedback helped me make better contact with the surface.*” However, one participant expressed reservations, stating that the feedback was somewhat exaggerated compared to real drawing: “*The vibration of the brush made it difficult to draw straight lines*” (P5).

d) Conclusion: In summary, qualitative feedback from participants shows that our device enhanced interaction in most VR scenarios without imposing additional burdens. Participants did not report noticeable hand discomfort over extended use, and the device did not interfere with fine motor control of the hand.

X. FUTURE WORK

The focus of this paper has been on developing a highly integrated and flexible user-customized electro-haptic device capable of delivering precise and multi-dimensional feedback. While the current study demonstrates the feasibility and effectiveness of our approach, there is room for follow-up research and exploration.

a) Multi-modality feedback integration: Our current device primarily provides electro-haptic feedback. Future works could integrate additional modalities such as thermal feedback (temperature cues) and mechanical feedback (e.g., pressure or vibration). Combining these modalities would enable richer

and more immersive haptic experiences, further enhancing realism in virtual and augmented environments.

b) Sensor integration for enhanced interaction: Incorporating integrated sensors (e.g., motion tracking, force sensing, or bio-signals such as EMG/EEG) into the device would allow for more precise detection of hand position, gestures, and fine motor control. Such functionality could be particularly useful when visual tracking is limited—for example, in low-light conditions or when the user’s hands are out of camera of headset, supporting accurate reconstruction of hand interactions in virtual spaces.

c) Applications in AR and XR: While the present work focuses on VR scenarios, extending the device to augmented reality (AR) and extended reality (XR) applications would broaden its potential impact. In AR, for example, the device could support tactile cues for interacting with virtual overlays on real-world objects, while in XR it could contribute to hybrid workspaces, medical simulations, or remote collaboration environments where precise tactile cues are important.

XI. CONCLUSION

We introduced a untethered, ultra-thin, and user-customized electro-haptic device that advances immersive human–machine interaction. Fabricated with soft silicone substrates and printable liquid metal-montmorillonite ink , the device conforms to the hand while remaining lightweight and minimally interfering. A palm-wide, addressable electrode array combined with waveform modulation enables spatially precise, fine-grained, and multi-dimensional haptic feedback.

Our user studies demonstrate that: (1) the electro-haptic device introduces minimal interference with hand movement and remains comfortable for extended wear; (2) it provides fine-grained, multi-dimensional, and variable electro-haptic sensations; and (3) it enhances interaction in most VR scenarios without imposing additional burdens. Furthermore, we show that the device can improve task performance and serve as an effective tool for haptic augmentation in VR applications. We believe that our electro-haptic device can be applied to a broader range of human–computer interaction scenarios and contribute to the advancement of next-generation haptic technologies.

ACKNOWLEDGMENT

This work was supported by National Natural Science Foundation of China (22574106, T2522023), the Science and Technology Commission of Shanghai Municipality (24490710900), and ShanghaiTech University (2023F0209-000-02).

REFERENCES

- [1] Jose Daniel Azofeifa, Julieta Noguez, Sergio Ruiz, José Martín Molina-Espinosa, Alejandra J. Magana, and Bedrich Benes. Systematic review of multimodal human–computer interaction. *Informatics*, 9(1), 2022.
- [2] Eloy Irigoyen, Mikel Larrea, and Manuel Graña. A narrative review of haptic technologies and their value for training, rehabilitation, and the education of persons with special needs. *Sensors (Basel, Switzerland)*, 24(21):6946, 2024.
- [3] Sebastian Vizcay, Panagiotis Kourtesis, Ferran Argelaguet, Claudio Pacchierotti, and Maud Marchal. Electrotactile feedback for enhancing contact information in virtual reality. *arXiv preprint arXiv:2102.00259*, 2021.
- [4] Xian Wang, Diego Monteiro, Lik-Hang Lee, Pan Hui, and Hai-Ning Liang. Vibroweight: Simulating weight and center of gravity changes of objects in virtual reality for enhanced realism. In *2022 IEEE haptics symposium (HAPTICS)*, pages 1–7. IEEE, 2022.
- [5] M Reza Motamedi, Jean-Philippe Roberge, and Vincent Duchaine. The use of vibrotactile feedback to restore texture recognition capabilities, and the effect of subject training. *IEEE Transactions on Neural Systems and Rehabilitation Engineering*, 25(8):1230–1239, 2016.
- [6] Unnikrishnan Radhakrishnan, Lisheng Kuang, Konstantinos Koumaditis, Francesco Chinello, and Claudio Pacchierotti. Haptic feedback, performance and arousal: A comparison study in an immersive vr motor skill training task. *IEEE transactions on haptics*, 17(2):249–262, 2023.
- [7] Panagiotis Kourtesis, Sebastian Vizcay, Maud Marchal, Claudio Pacchierotti, and Ferran Argelaguet. Action-specific perception & performance on a fitts’s law task in virtual reality: The role of haptic feedback. *IEEE Transactions on Visualization and Computer Graphics*, 28(11):3715–3726, 2022.
- [8] Yunxiang Zhang, Benjamin Liang, Boyuan Chen, Paul M Torrens, S Farokh Atashzar, Dahua Lin, and Qi Sun. Force-aware interface via electromyography for natural vr/ar interaction. *ACM Transactions on Graphics (TOG)*, 41(6):1–18, 2022.
- [9] Jessica Yin, Ronan Hinchet, Herbert Shea, and Carmel Majidi. Wearable soft technologies for haptic sensing and feedback. *Advanced Functional Materials*, 31(39):2007428, 2021.
- [10] Joshua J Fleck, Zane A Zook, Janelle P Clark, Daniel J Preston, Darren J Lipomi, Claudio Pacchierotti, and Marcia K O’Malley. Wearable multi-sensory haptic devices. *Nature Reviews Bioengineering*, pages 1–15, 2025.
- [11] Yuyu Gao, Kuanming Yao, Shengxin Jia, Ya Huang, Guangyao Zhao, Binbin Zhang, Yiming Liu, and Xinge Yu. Advances in materials for haptic skin electronics. *Matter*, 7(9):2826–2845, 2024.
- [12] Bingjian Huang, Paul H Dietz, and Daniel Wigdor. Investigating the effects of intensity and frequency on vibrotactile spatial acuity. *IEEE Transactions on Haptics*, 17(3):405–416, 2024.
- [13] Ziliang Zhou, Yicheng Yang, Jinbiao Liu, Jia Zeng, Xiaoxin Wang, and Honghai Liu. Electrotactile perception properties and its applications: A review. *IEEE transactions on haptics*, 15(3):464–478, 2022.
- [14] Rahul Kumar Ray, Madhan Kumar Vasudevan, and M Manivannan. Electrotactile displays: taxonomy, cross-modality, psychophysics and challenges. *Frontiers in Virtual Reality*, 5:1406923, 2024.

- [15] Keigo Ushiyama and Pedro Lopes. Feetthrough: electro-tactile foot interface that preserves real-world sensations. In *Proceedings of the 36th Annual ACM Symposium on User Interface Software and Technology*, pages 1–11, 2023.
- [16] Kyeonghee Lim, Hunkyu Seo, Won Gi Chung, Hayoung Song, Myoungjae Oh, Seoung Young Ryu, Younhee Kim, and Jang-Ung Park. Material and structural considerations for high-performance electrodes for wearable skin devices. *Communications Materials*, 5(1):49, 2024.
- [17] Mingyu Kim, Changyu Jeon, and Jinmo Kim. A Study on Immersion and Presence of a Portable Hand Haptic System for Immersive Virtual Reality. *Sensors*, 17(5):1141, May 2017.
- [18] Eleftherios Triantafyllidis, Christopher Mcgreavy, Ji-acheng Gu, and Zhibin Li. Study of Multimodal Interfaces and the Improvements on Teleoperation. *IEEE Access*, 8:78213–78227, 2020.
- [19] Shan-Yuan Teng, Pengyu Li, Romain Nith, Joshua Fonseca, and Pedro Lopes. Touch&Fold: A Foldable Haptic Actuator for Rendering Touch in Mixed Reality. In *Proceedings of the 2021 CHI Conference on Human Factors in Computing Systems*, pages 1–14, Yokohama Japan, May 2021. ACM.
- [20] Xiaobin Ji, Xinchang Liu, Vito Cacucciolo, Yoan Civet, Alae El Haitami, Sophie Cantin, Yves Perriard, and Herbert Shea. Untethered Feel-Through Haptics Using 18- μm Thick Dielectric Elastomer Actuators. *Advanced Functional Materials*, 31(39):2006639, September 2021.
- [21] Ulrike Gollner, Tom Bieling, and Gesche Joost. Mobile Lorm Glove: introducing a communication device for deaf-blind people. In *Proceedings of the Sixth International Conference on Tangible, Embedded and Embodied Interaction*, pages 127–130, Kingston Ontario Canada, February 2012. ACM.
- [22] Nicholas Caporusso. A wearable Malossi alphabet interface for deafblind people. In *Proceedings of the working conference on Advanced visual interfaces*, pages 445–448, Napoli Italy, May 2008. ACM.
- [23] Oliver Ozioko, William Taube, Marion Hersh, and Ravinder Dahiya. SmartFingerBraille: A tactile sensing and actuation based communication glove for deafblind people. In *2017 IEEE 26th International Symposium on Industrial Electronics (ISIE)*, pages 2014–2018, Edinburgh, United Kingdom, June 2017. IEEE.
- [24] Dengfeng Li, Jiahui He, Zhen Song, Kuanming Yao, Mengge Wu, Haoran Fu, Yiming Liu, Zhan Gao, Jingkun Zhou, Lei Wei, Zhengyou Zhang, Yuan Dai, Zhaoqian Xie, and Xinge Yu. Miniaturization of mechanical actuators in skin-integrated electronics for haptic interfaces. *Microsystems & Nanoengineering*, 7(1):85, October 2021.
- [25] Xinge Yu, Zhaoqian Xie, Yang Yu, Jungyup Lee, Abraham Vazquez-Guardado, Haiwen Luan, Jasper Ruban, Xin Ning, Aadeel Akhtar, Dengfeng Li, Bowen Ji, Yiming Liu, Rujie Sun, Jingyue Cao, Qingze Huo, Yishan Zhong, ChanMi Lee, SeungYeop Kim, Philipp Gutruf, Changxing Zhang, Yeguang Xue, Qinglei Guo, Aditya Chempakasseril, Peilin Tian, Wei Lu, JiYoon Jeong, YongJoon Yu, Jesse Cornman, CheeSim Tan, BongHoon Kim, KunHyuk Lee, Xue Feng, Yonggang Huang, and John A. Rogers. Skin-integrated wireless haptic interfaces for virtual and augmented reality. *Nature*, 575(7783):473–479, November 2019.
- [26] Ronan Hinchet, Velko Vechev, Herbert Shea, and Otmar Hilliges. DextriES: Wearable Haptic Feedback for Grasping in VR via a Thin Form-Factor Electrostatic Brake. In *Proceedings of the 31st Annual ACM Symposium on User Interface Software and Technology*, pages 901–912, Berlin Germany, October 2018. ACM.
- [27] Cathy Fang, Yang Zhang, Matthew Dworman, and Chris Harrison. Wireality: Enabling Complex Tangible Geometries in Virtual Reality with Worn Multi-String Haptics. In *Proceedings of the 2020 CHI Conference on Human Factors in Computing Systems*, pages 1–10, Honolulu HI USA, April 2020. ACM.
- [28] Ryohei Michikawa, Takahiro Endo, and Fumitoshi Matsuno. A Multi-DoF Exoskeleton Haptic Device for the Grasping of a Compliant Object Adapting to a User’s Motion Using Jamming Transitions. *IEEE Transactions on Robotics*, 39(1):373–385, February 2023.
- [29] J. Blake and H.B. Gurocak. Haptic Glove With MR Brakes for Virtual Reality. *IEEE/ASME Transactions on Mechatronics*, 14(5):606–615, October 2009.
- [30] Harshal Arun Sonar and Jamie Paik. Soft Pneumatic Actuator Skin with Piezoelectric Sensors for Vibrotactile Feedback. *Frontiers in Robotics and AI*, 2, January 2016.
- [31] Harshal A. Sonar, Aaron P. Gerratt, Stéphanie P. Lacour, and Jamie Paik. Closed-Loop Haptic Feedback Control Using a Self-Sensing Soft Pneumatic Actuator Skin. *Soft Robotics*, 7(1):22–29, February 2020.
- [32] Vito Cacucciolo, Jun Shintake, Yu Kuwajima, Shingo Maeda, Dario Floreano, and Herbert Shea. Stretchable pumps for soft machines. *Nature*, 572(7770):516–519, August 2019.
- [33] Vivian Shen, Tucker Rae-Grant, Joe Mullenbach, Chris Harrison, and Craig Shultz. Fluid Reality: High-Resolution, Untethered Haptic Gloves using Electroosmotic Pump Arrays. In *Proceedings of the 36th Annual ACM Symposium on User Interface Software and Technology*, pages 1–20, San Francisco CA USA, October 2023. ACM.
- [34] Seung-Chan Kim, Chong-Hui Kim, Gi-Hun Yang, Tae-Heon Yang, Byung-Kil Han, Sung-Chul Kang, and Dong-Soo Kwon. Small and lightweight tactile display(SaLT) and its application. In *World Haptics 2009 - Third Joint EuroHaptics conference and Symposium on Haptic Interfaces for Virtual Environment and Teleoperator Systems*, pages 69–74, Salt Lake City, UT, USA, March 2009. IEEE.
- [35] Qi Wang and V. Hayward. Compact, Portable, Modular, High-performance, Distributed Tactile Transducer Device

- Based on Lateral Skin Deformation. In *2006 14th Symposium on Haptic Interfaces for Virtual Environment and Teleoperator Systems*, pages 67–72, Alexandria, VA, USA, 2006. IEEE.
- [36] Minglu Zhu, Zhongda Sun, Zixuan Zhang, Qiongfeng Shi, Tianyi He, Huicong Liu, Tao Chen, and Chengkuo Lee. Haptic-feedback smart glove as a creative human-machine interface (HMI) for virtual/augmented reality applications. *Science Advances*, 6(19):eaaz8693, May 2020.
 - [37] Mitsuru Nakajima, Keisuke Hasegawa, Yasutoshi Makino, and Hiroyuki Shinoda. Spatiotemporal Pinpoint Cooling Sensation Produced by Ultrasound-Driven Mist Vaporization on Skin. *IEEE Transactions on Haptics*, 14(4):874–884, October 2021.
 - [38] Euan Freeman and Graham Wilson. Perception of Ultrasound Haptic Focal Point Motion. In *Proceedings of the 2021 International Conference on Multimodal Interaction*, pages 697–701, Montréal QC Canada, October 2021. ACM.
 - [39] Benjamin Long, Sue Ann Seah, Tom Carter, and Sriram Subramanian. Rendering volumetric haptic shapes in mid-air using ultrasound. *ACM Transactions on Graphics*, 33(6):1–10, November 2014.
 - [40] K.A. Kaczmarek, J.G. Webster, P. Bach-y Rita, and W.J. Tompkins. Electrotactile and vibrotactile displays for sensory substitution systems. *IEEE Transactions on Biomedical Engineering*, 38(1):1–16, January 1991.
 - [41] Hiroyuki Kajimoto, Naoki Kawakami, Taro Maeda, and Susumu Tachi. Tactile Feeling Display using Functional Electrical Stimulation.
 - [42] Yei Hwan Jung, Jae-Hwan Kim, and John A. Rogers. Skin-Integrated Vibrohaptic Interfaces for Virtual and Augmented Reality (Adv. Funct. Mater. 39/2021). *Advanced Functional Materials*, 31(39):2170291, September 2021.
 - [43] Arianna Mazzotta, Marco Carlotti, and Virgilio Mattoli. Conformable on-skin devices for thermo-electro-tactile stimulation: materials, design, and fabrication. *Materials Advances*, 2(6):1787–1820, 2021.
 - [44] M. Ercan Altinsoy and Sebastian Merchel. Electrotactile Feedback for Handheld Devices with Touch Screen and Simulation of Roughness. *IEEE Transactions on Haptics*, 5(1):6–13, January 2012.
 - [45] Vibol Yem, Kevin Vu, Yuki Kon, and Hiroyuki Kajimoto. Effect of Electrical Stimulation Haptic Feedback on Perceptions of Softness-Hardness and Stickiness While Touching a Virtual Object. In *2018 IEEE Conference on Virtual Reality and 3D User Interfaces (VR)*, pages 89–96, Reutlingen, March 2018. IEEE.
 - [46] Michele Germani, Maura Mengoni, and Margherita Peruzzini. Electro-tactile device for material texture simulation. *The International Journal of Advanced Manufacturing Technology*, 68(9-12):2185–2203, October 2013.
 - [47] Colin V. Keef, Laure V. Kayser, Stazia Tronboll, Cody W. Carpenter, Nicholas B. Root, Mickey Finn, Timothy F. O'Connor, Sami N. Abuhamdieh, Daniel M. Davies, Rory Runser, Ying Shirley Meng, Vilayanur S. Ramachandran, and Darren J. Lipomi. Virtual Texture Generated Using Elastomeric Conductive Block Copolymer in a Wireless Multimodal Haptic Glove. *Advanced Intelligent Systems*, 2(4):2000018, April 2020.
 - [48] Yahya Abbass, Strahinja Dosen, Lucia Seminara, and Maurizio Valle. Full-hand electrotactile feedback using electronic skin and matrix electrodes for high-bandwidth human-machine interfacing. *Philosophical Transactions of the Royal Society A: Mathematical, Physical and Engineering Sciences*, 380(2228):20210017, July 2022.
 - [49] Weikang Lin, Dongsheng Zhang, Wang Wei Lee, Xuelong Li, Ying Hong, Qiqi Pan, Ruirui Zhang, Guoxiang Peng, Hong Z. Tan, Zhengyou Zhang, Lei Wei, and Zhengbao Yang. Super-resolution wearable electrotactile rendering system. *Science Advances*, 8(36):eabp8738, September 2022.
 - [50] Devin Murphy, Yichen Li, Crystal Elaine Owens, Layla Stanton, Paul Pu Liang, Yiyue Luo, Antonio Torralba, and Wojciech Matusik. Fits like a flex-glove: Automatic design of personalized fpcb-based tactile sensing gloves. In *Proceedings of the Extended Abstracts of the CHI Conference on Human Factors in Computing Systems*, CHI EA '25, New York, NY, USA, 2025. Association for Computing Machinery.
 - [51] Ismail Ben Abdallah, Yassine Bouteraa, and Chokri Rekik. Design and development of 3d printed myoelectric robotic exoskeleton for hand rehabilitation. *International journal on smart sensing and intelligent systems*, 10(2):341, 2017.
 - [52] Nicola Secciani, Chiara Brogi, Marco Pagliai, Francesco Buonomici, Filippo Gerli, Federica Vannetti, Massimo Bianchini, Yary Volpe, and Alessandro Ridolfi. Wearable robots: An original mechatronic design of a hand exoskeleton for assistive and rehabilitative purposes. *Frontiers in Neurorobotics*, 15:750385, 2021.
 - [53] Anik Kumar Saha, Md Abrar Jahin, Md Rafiquzzaman, and Muhammad Firoz Mridha. Ergonomic design of computer laboratory furniture: Mismatch analysis utilizing anthropometric data of university students. *Heliyon*, 10(14), 2024.
 - [54] Daniele Esposito, Jessica Centracchio, Emilio Andreozzi, Sergio Savino, Gaetano D Gargiulo, Ganesh R Naik, and Paolo Bifulco. Design of a 3d-printed hand exoskeleton based on force-myography control for assistance and rehabilitation. *Machines*, 10(1):57, 2022.
 - [55] Yudai Tanaka, Alan Shen, Andy Kong, and Pedro Lopes. Full-hand electro-tactile feedback without obstructing palmar side of hand. In *Proceedings of the 2023 CHI Conference on Human Factors in Computing Systems*, CHI '23, New York, NY, USA, 2023. Association for Computing Machinery.
 - [56] Anusha Withana, Daniel Groeger, and Jürgen Steimle. Tacttoo: A thin and feel-through tattoo for on-skin tactile output. In *Proceedings of the 31st Annual ACM*

- Symposium on User Interface Software and Technology*, UIST '18, page 365–378, New York, NY, USA, 2018. Association for Computing Machinery.
- [57] Mei-ying Kwan, Kit-lun Yick, Lung Chow, Annie Yu, Sun-pui Ng, and Joanne Yip. Impact of postural variation on hand measurements: Three-dimensional anatomical analysis. *PLoS one*, 16(4):e0250428, 2021.
 - [58] Clayton Leite, Petr Byvshev, Henry Mauranen, and Yu Xiao. Simulation-driven design of smart gloves for gesture recognition. *Scientific Reports*, 14(1):14873, 2024.
 - [59] Weiya Chen, Chenchen Yu, Chenyu Tu, Zehua Lyu, Jing Tang, Shiqi Ou, Yan Fu, and Zhidong Xue. A survey on hand pose estimation with wearable sensors and computer-vision-based methods. *Sensors*, 20(4):1074, 2020.
 - [60] Javier Romero, Dimitrios Tzionas, and Michael J. Black. Embodied hands: Modeling and capturing hands and bodies together. *ACM Transactions on Graphics, (Proc. SIGGRAPH Asia)*, 36(6), November 2017.
 - [61] Xiong Zhang, Qiang Li, Hong Mo, Wenbo Zhang, and Wen Zheng. End-to-end hand mesh recovery from a monocular rgb image. 2019.
 - [62] Hanwen Jiang, Shaowei Liu, Jiashun Wang, and Xiaolong Wang. Hand-object contact consistency reasoning for human grasps generation. In *Proceedings of the International Conference on Computer Vision*, 2021.
 - [63] Baowen Zhang, Yangang Wang, Xiaoming Deng, Yinda Zhang, Ping Tan, Cuixia Ma, and Hongan Wang. Interacting two-hand 3d pose and shape reconstruction from single color image. In *Proceedings of the IEEE/CVF International Conference on Computer Vision (ICCV)*, pages 11354–11363, October 2021.
 - [64] Xingyu Chen, Yufeng Liu, Chongyang Ma, Jianlong Chang, Huayan Wang, Tian Chen, Xiaoyan Guo, Pengfei Wan, and Wen Zheng. Camera-space hand mesh recovery via semantic aggregation and adaptive 2d-1d registration. In *Proceedings of the IEEE/CVF Conference on Computer Vision and Pattern Recognition (CVPR)*, pages 13274–13283, June 2021.
 - [65] Xingyu Chen, Yufeng Liu, Dong Yajiao, Xiong Zhang, Chongyang Ma, Yanmin Xiong, Yuan Zhang, and Xiaoyan Guo. Mobrecon: Mobile-friendly hand mesh reconstruction from monocular image. In *Proceedings of the IEEE/CVF Conference on Computer Vision and Pattern Recognition (CVPR)*, 2022.
 - [66] Pengfei Xie, Wenqiang Xu, Tutian Tang, Zhenjun Yu, and Cewu Lu. Ms-mano: Enabling hand pose tracking with biomechanical constraints. In *Proceedings of the IEEE/CVF conference on computer vision and pattern recognition*, pages 2382–2392, 2024.
 - [67] Ziwei Yu, Chen Li, Linlin Yang, Xiaoxu Zheng, Michael Bi Mi, Gim Hee Lee, and Angela Yao. Overcoming the trade-off between accuracy and plausibility in 3d hand shape reconstruction. In *Proceedings of the IEEE/CVF conference on computer vision and pattern recognition*, pages 544–553, 2023.
 - [68] Yu Lei, Yi Deng, Lin Dong, Xiaohui Li, Xiangnan Li, and Zhi Su. A novel sensor fusion approach for precise hand tracking in virtual reality-based human–computer interaction. *Biomimetics*, 8(3):326, 2023.
 - [69] Xingyu Chen, Yufeng Liu, Yajiao Dong, Xiong Zhang, Chongyang Ma, Yanmin Xiong, Yuan Zhang, and Xiaoyan Guo. Mobrecon: Mobile-friendly hand mesh reconstruction from monocular image. In *Proceedings of the IEEE/CVF conference on computer vision and pattern recognition*, pages 20544–20554, 2022.
 - [70] Shantonu Biswas and Yon Visell. Emerging material technologies for haptics. *Advanced Materials Technologies*, 4(4):1900042, 2019.
 - [71] Yufeng Qin, Xueqiong Ouyang, Yang Lv, Wencai Liu, Qing Liu, and Shuangxi Wang. A review of carbon-based conductive inks and their printing technologies for integrated circuits. *Coatings*, 13(10):1769, 2023.
 - [72] Vicente Orts Mercadillo, Kai Chio Chan, Mario Caironi, Athanassia Athanassiou, Ian A Kinloch, Mark Bissett, and Pietro Cataldi. Electrically conductive 2d material coatings for flexible and stretchable electronics: a comparative review of graphenes and mxenes. *Advanced Functional Materials*, 32(38):2204772, 2022.
 - [73] Leily Majidi, Dmitry Gritsenko, and Jie Xu. Gallium-based room-temperature liquid metals: Actuation and manipulation of droplets and flows. *Frontiers in Mechanical Engineering*, 3:9, 2017.
 - [74] Yifan Deng, Fan Bu, Yujie Wang, Pei Song Chee, Xiangye Liu, and Cao Guan. Stretchable liquid metal based biomedical devices. *npj Flexible Electronics*, 8(1):12, 2024.
 - [75] Michael D Dickey. Stretchable and soft electronics using liquid metals. *Advanced materials*, 29(27):1606425, 2017.
 - [76] Wuzhou Zu, Hugo E Carranza, and Michael D Bartlett. Enhancing electrical conductivity of stretchable liquid metal–silver composites through direct ink writing. *ACS Applied Materials & Interfaces*, 16(18):23895–23903, 2024.
 - [77] Yiran Ding, Mengqi Zeng, and Lei Fu. Surface chemistry of gallium-based liquid metals. *Matter*, 3(5):1477–1506, 2020.
 - [78] Ziang Cui, Yiqing Zhang, Siyuan Chen, Xingming Wen, Yining Zhao, Yitao Ma, Qihang Yan, Zixiong Wu, Yuxi He, Guohui Wang, et al. A printable liquid metal–montmorillonite ink for high-resolution stretchable bioelectronics. *Journal of Materials Chemistry C*, 2025.
 - [79] Hao Wu, Ganguang Yang, Kanhai Zhu, Shaoyu Liu, Wei Guo, Zhuo Jiang, and Zhuo Li. Materials, devices, and systems of on-skin electrodes for electrophysiological monitoring and human–machine interfaces. *Advanced Science*, 8(2):2001938, 2021.
 - [80] Hailing Xue, Dongyang Wang, Mingyan Jin, Hanbing Gao, Xuhui Wang, Long Xia, Dong'ang Li, Kai Sun, Huanan Wang, Xufeng Dong, et al. Hydrogel elec-

- trodes with conductive and substrate-adhesive layers for noninvasive long-term eeg acquisition. *Microsystems & Nanoengineering*, 9(1):79, 2023.
- [81] Yulin Fu, Jingjing Zhao, Ying Dong, and Xiaohao Wang. Dry electrodes for human bioelectrical signal monitoring. *Sensors*, 20(13):3651, 2020.
 - [82] Stefan Manoharan and Hangue Park. Characterization of perception by transcutaneous electrical stimulation in terms of tingling intensity and temporal dynamics. *Biomedical Engineering Letters*, 14(1):35–44, 2024.
 - [83] Michael R Zemaitis, Lissa A Foris, Richard A Lopez, and Martin R Huecker. Electrical injuries. 2017.